Adsorption of Cr^{6+} and Pb^{2+} on Soy Sauce Residue Biochar from Aqueous Solution

Xiaoxun Xu,[a,b,#] Chenying Zhou,[a,#] Shirong Zhang,[a,b,*] Zhang Cheng,[a] Zhanbiao Yang,[a] Junren Xian,[a] and Yuanxiang Yang [a]

Biochar produced by the pyrolysis of biomass can be used to counter water pollution from heavy metals. The purpose of this work was to develop a biosorbent based on soy sauce residue (SSR) for the removal of Cr^{6+} and Pb^{2+}. The SSR biochar (SBC) from oxygen-limited pyrolysis under the temperatures of 300 to 700 °C were obtained, and their adsorption capability was evaluated. After determining the optimum pyrolysis temperature, the effects of initial pH values, contact times, and initial metal concentrations on the Cr^{6+} and Pb^{2+} adsorption by SBC prepared at 600 °C (SBC600) were investigated. With the increase of pyrolysis temperature, the physical and chemical properties of SBC developed in a direction favorable to heavy metal adsorption. The SBC600 reached the adsorption equilibrium at the time of 2 (Cr^{6+}) and 24 h (Pb^{2+}), and the maximum adsorption amounts of Cr^{6+} and Pb^{2+} were 25.80 and 135.3 mg/g, respectively. The adsorption kinetics followed the pseudo-second-order kinetic equation, and the adsorption isotherms was best described by the Langmuir isotherms. The SBC was an adsorbent with certain potential for heavy metals removal in wastewater.

Keywords: Soy sauce residue biochar; Adsorption; Heavy metal; Kinetics; Thermodynamics

*Contact information: a: School of Environment Sciences, Sichuan Agricultural University, Chengdu, 611130, China; b: Key Laboratory of Soil Environment Protection of Sichuan Province, Sichuan Agricultural University, Chengdu, 611130, China; #: These authors contributed equally to this work and should be considered co-first authors; *Corresponding authors: srzhang01@aliyun.com*

INTRODUCTION

Water pollution by heavy metals has become a major concern worldwide due to improper disposal of solid waste, smelting, mining, sewage irrigation, abuse of chemical fertilizers, and pesticides (Guan and Sun 2014). The toxic metals ions, such as Cr^{6+} and Pb^{2+}, generally coexist in contaminated waters and some industrial effluents (Shaw and Dussan 2017; Diao *et al*. 2018). As the main sources of contamination toxicity in wastewater, they could threaten human health through direct drinking, skin contact, or through the food chain (Izah *et al*. 2016). Therefore, it is urgent to apply an eco-friendly and feasible method to remove Cr^{6+} and Pb^{2+} from wastewater.

At present, the common treatment technologies of heavy metal in wastewater include coagulation flocculation, biological treatment, and adsorption methods (Lee *et al*. 2015; Brahmi *et al*. 2017; Kiran *et al*. 2017). Researchers have paid more attention to adsorption methods in the last years due to high adsorption efficiency, simplicity, less secondary pollution, and selectivity (Meng *et al*. 2019). Biochar is an adsorption material with high adsorption efficiency and low cost (Amin *et al*. 2017). Moreover, the biochar from waste residue used to remove heavy metal in wastewater can solve the problem of waste recycling to a large extent (Fan *et al*. 2018).

Soy sauce residue (SSR) from the sauce production process is often treated as fertilizer, feed, or garbage because it is difficult to transport and unsuitable for storage. It will not only cause a loss of resources, but also lead to environmental pollution (Li *et al*. 2013). The SSR is rich in coarse protein and fat, crude fiber of plant, and isoflavones. It can be used in the simultaneous extraction of oil and soy isoflavones and carbon source for sludge conditioning (Chen *et al*. 2014b; Duan *et al*. 2019). There has been a need for research on the preparation of biochar from SSR, while the problem of SSR loss and environmental pollution can be solved well by using it as the raw material of biochar.

The authors assumed that SSR was a potential material to prepare the biochar and that soy sauce residue biochar (SBC) could be effective for the adsorption of heavy metals in wastewater. However, little evidence is available for this hypothesis. Therefore, the specific purposes of this study were (1) to provide an adsorbent for the Cr^{6+} and Pb^{2+} in aqueous solution; (2) to investigate the effects of initial pH, contact time, and initial metal concentration on SBC for adsorption of Cr^{6+} and Pb^{2+}; and (3) to discuss the possible mechanism of SBC for Cr^{6+} and Pb^{2+} removal. It is expected that this study can provide useful data to maximize the beneficial use of SBC as an effective biosorbent for Cr^{6+} and Pb^{2+} removal. Furthermore, the research would help the authors to develop a novel application strategy to suitably manage renewable solid waste by recycling them into the environment.

EXPERIMENTAL

Materials and Reagents

The SSR was supplied by a brewing enterprise (Qianhe Condiment and Food Co., Ltd.) of Chengdu, China. After the removal of the dust on the surface of SSR, it was air-dried at room temperature and then smashed to pass through a 20-mesh sieve (0.90 mm) and preserved as the raw material.

Lead nitrate ($Pb(NO_3)_2$), potassium dichromate ($K_2Cr_2O_7$), nitric acid (HNO_3), and sodium hydroxide (NaOH) were purchased commercially (analytical reagent grade, Sichuan YaHua Industrial Group Co., Ltd, Chengdu, China). A total of 1000 mg/L Cr^{6+} or Pb^{2+} stock solution was produced *via* dissolving K_2CrO_7 or $Pb(NO_3)_2$ in distilled water, respectively. The diverse concentrations of Cr^{6+} or Pb^{2+} solutions used in this study were acquired *via* diluting the stock solution.

Biochar preparation

The SBC was prepared through oxygen-limited pyrolysis. After it was filled in the closed ceramic crucible, the powder of SSR was placed in a furnace. The furnace was programmed to heat with a rate of 20 °C/min until it reached a specified temperature (300, 400, 500, 600, and 700 °C), and carbonization was completed at different pyrolysis temperatures for 2 h. After cooling to reach the room temperature, the SBC was removed and rinsed with ultra-pure water until the pH reached a stable state. The SBC was marked as SBC300, SBC400, SBC500, SBC600, and SBC700. After drying the SBC at 80 °C, then it was smashed to pass through a 100-mesh sieve (0.15 mm).

The productivity were determined by weighing the mass before and after pyrolysis, and the ash content were determined according to GB/T 12496.3 (1999), and the average aperture and specific surface area were determined *via* a multi-point Brunauer-Emmet-

Teller (BET) method. The SBC's basic physical and chemical properties are shown in Table 1.

Table 1. Basic Physical and Chemical Properties of SBC

Biochar	Productivity (%)	Ash Content (%)	Average Aperture (nm)	Total Pore Volume (m^2/g)	Microporous Specific Surface Area (m^2/g)	BET Surface Area (m^2/g)
SBC300	50.87	16.67	0.52	0.74	7.41	20.69
SBC400	34.47	26.25	2.08	1.69	70.85	100.77
SBC500	29.47	34.00	2.67	2.30	152.23	279.59
SBC600	23.73	42.33	3.59	2.28	94.15	196.44
SBC700	22.10	49.33	5.01	1.42	80.42	148.19

Methods

Characterizations of SBC

The appearance of SBC particles was observed *via* a scanning electron microscope (SEM; JSM-7500F; JEOL, Tokyo, Japan), and the functional groups of SBC were analyzed *via* FTIR (FTIR; Spectrum Two; PerkinElmer Inc., Waltham, MA, USA), and the elemental composition of SBC was determined using an elemental analyzer (Vario EL III; Elementar Analysen Systeme, Hanau, Germany).

Batch sorption experiment

The adsorption experiments were carried out in 50-mL centrifuge tubes, containing 80 mg of biochar sample and 40 mL of $K_2Cr_2O_7$ or $Pb(NO_3)_2$ solution. The ranges of experimental parameters were selected as follows: initial concentrations of $K_2Cr_2O_7$ (50-200 mg/L), initial concentrations of $Pb(NO_3)_2$ (50-200 mg/L), pH (1.0-6.0), and contact time (10-240 min for Cr^{6+} and 20-1440 min for Pb^{2+}). The pH was adjusted with 1% HNO_3 and 1% NaOH. The tubes were capped and shook in a constant temperature oscillator (25 °C, 200 r/min; KT-86A, Changzhou Zhongbei Instrument Co. Ltd., Changzhou, China). All treatments were replicated three times.

The removal and adsorption capacity of Cr^{6+} and Pb^{2+} after adsorption were calculated according to the following formulas,

$$p = \frac{C_0 - C_t}{C_0} \times 100\% \quad (1)$$

$$q_e = \frac{C_0 - C_t}{m} \times V \quad (2)$$

where p is the removal of Cr^{6+} and Pb^{2+} (%), q_e is the adsorption capacity of Cr^{6+} and Pb^{2+} (mg/g), C_0 is the initial concentration of Cr^{6+} and Pb^{2+} before adsorption (mg/L), C_t is the concentration of Cr^{6+} and Pb^{2+} after adsorption for t min (mg/L), m is the dosage of SBC, (g), and V is the volume of Cr^{6+} and Pb^{2+} solution (L).

Adsorption kinetics: The pseudo-first-order (Eq. 3) and pseudo-second-order (Eq. 4) kinetic models were used to describe the kinetics of adsorption of Cr^{6+} and Pb^{2+} by SBC,

$$q_t = q_e \times (1 - e^{-k_1 t}) \quad (3)$$

$$q_t = \frac{tk_2 q_e^2}{1+tk_2 q_e} \quad (4)$$

where q_e is the equilibrium adsorption amount (mg/g), q_t is the adsorption amount of SBC for heavy metals (mg/g) at time t (min), k_1 is the constant of reaction rate of the pseudo-first-order kinetic model (/min), and k_2 is the constant of reaction rate of the pseudo-second-order kinetic model (g/(mg • min)).

Adsorption isotherm equation: Langmuir equation (Eq. 5) and Freundlich equation (Eq. 6) were used to fit the experimental results. The equations are as follows,

$$Q_e = \frac{K_L Q_m C_e}{1+K_L C_e} \quad (5)$$

$$Q_e = K_f (C_e)^n \quad (6)$$

where Q_e is the equilibrium adsorption amount (mg/g), Q_m is the maximum adsorption amount (mg/g), C_e is the equilibrium concentration of Cr^{6+} in the solution (mg/L), K_L is the constant of Langmuir adsorption equilibrium (L/mg), K_f is the empirical Freundlich constants related to sorption capacity, and n is the empirical Freundlich constant related to sorption intensity.

The solution was centrifugally filtrated after adsorption, and the Cr^{6+} concentration was analyzed using 1,5-diphenylcarbazide colorimetric method by measuring the absorbance at 540 nm in the filtrate with a UV-vis spectrophotometer (UV-1780, Shimadzu, Co. Ltd., Shanghai, China). The concentration of Pb^{2+} in the filtrate was determined via flame atomic absorption spectrophotometry (Thermo Solaar M6; Thermo Fisher Scientific, Ltd., Waltham, MA, USA).

Data Processing

The data were analyzed by Statistical Product and Service Solutions 22.0 (SPSS Institute Inc., Chicago, IL, USA), including a single factor analysis of variance (ANOVA), relationship modeling of influencing factors, descriptive statistics, and comparisons of significance difference between treatments conducted by least significant difference (LSD). Data analysis was performed using Origin 9.1 (OriginLab, Origin 9.1, Northampton, MA, USA). The data are the average values of three repetitions.

RESULTS AND DISCUSSION

Structure Characterization and Physicochemical Properties of Biochar Prepared at Different Temperatures

FITR spectra

The preparation temperature has a great influence on the surface functional groups of biochar (Zhang *et al.* 2013). The Fourier infrared spectrum of five kinds of biochar prepared at different temperatures is shown in Fig. 1. They had strong absorption peaks at 3432, 2874, 1607, 1102, and 832 cm^{-1}. The appearance of an absorption peak located at 3432 cm^{-1} was due to –OH, which might be derived from carbohydrates in organic matter (Wu *et al*. 2017). The characteristic peak at 2874 cm^{-1} was attributed to the symmetric and asymmetric stretching vibration of $-CH_2$ of aliphatic hydrocarbon and the characteristic

absorption peak of benzene ring was 1607 cm^{-1}. The absorption peak appearing at approximately 1102 cm^{-1} was produced by the stretching vibration of C-O, which indicated that SBC might contain surface groups such as ether bonds, alcohols, and lipids. In addition, the absorption peak at 832 cm^{-1} could be attributed to the stretching deformation vibration of the C-H in aromatic compounds (Lammers *et al*. 2009).

It could be seen from the FTIR spectrum that the SBC was mainly composed of an aromatic skeleton and contained functional groups, such as the hydroxyl group and the aromatic ether. As the pyrolysis temperature increased, the groups that SBC contained were slightly different, but only SBC prepared at 300 °C contained -CH_2, and SBC600 and SBC700 showed a C-O (Fig. 1). This phenomenon indicated that as the pyrolysis temperature increased, the alkyl group was deleted, and the degree of aromatization of biochar gradually increased. The main reason for this phenomenon was that the increase of temperature caused the break of C-C, C-O, and C-H bonds in the cellulose molecules, and various free radicals formed. After a series of cyclization reactions and collisions, these radicals formed –OH and other functional groups. These groups provided sites for the binding of heavy metal cations. Thereby, they provided a basis for the adsorption of heavy metal ions by SBC (Zhang *et al*. 2016). In addition, the presence of C-O ether bond groups increased the adsorption and ion exchange capacity of biochar for heavy metals (Radwan *et al*. 2010). Therefore, the presence of an ether bond in SBC600 and SBC700 indicated that they had good adsorption potential for heavy metal ions.

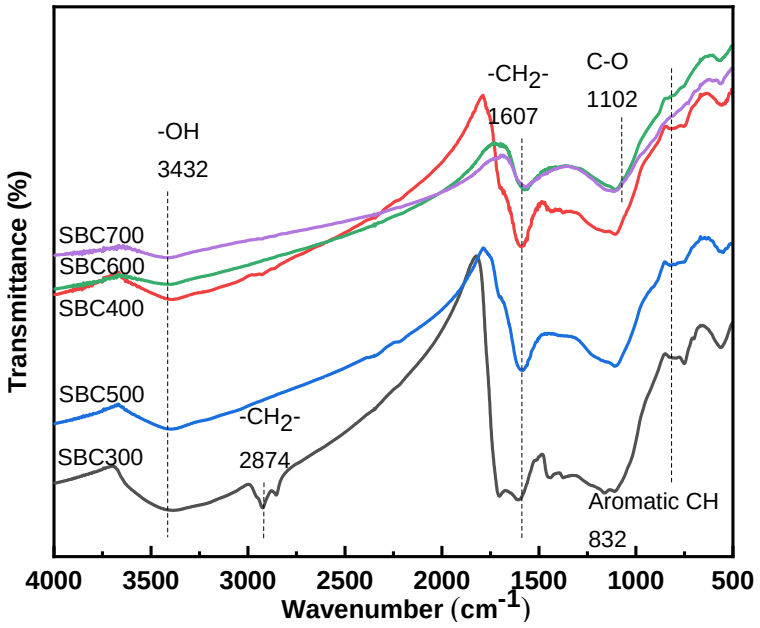

Fig. 1. Infrared spectrum of biochar at different pyrolysis temperatures

SEM analyses

The scanning electron micrograph group visually reflected the pore variation of the biochar surface prepared at different pyrolysis temperatures (Hamza *et al*. 2016). In this study, the pores exhibited by the SBC were mostly transverse tubular structures (Fig. 2). Under low temperature conditions (< 400 °C), SBC was at the degree of low carbonization and had few pore structure and small pores. When the pyrolysis temperature exceeded 400 °C, the pore structure of the SBC surface gradually formed, and the tubular structure

began to deform remarkably. From the results shown in Fig. 2, the fiber structure of SBC600 and SBC700 were broken, exhibiting an irregular pore-like structure that became looser, and the surface roughness was noticeably increased. However, the surface porosity of the biochar was reduced when the pyrolysis temperature was as high as 700 °C.

As the preparation temperature increased from 300 °C to 400 °C, the formation of large pores in SBC might have resulted from the honeycomb structure of soybean fiber in the SSR. As the preparation temperature continued to increase, more volatile mass escaped from SBC to form a distinctly porous structure (Wang *et al*. 2018a). On the one hand, the presence of these micropores provided sufficient contact between the biochar and the water sample. In contrast, it also provided a large number of heavy metal adsorption sites, which provided an ideal environment of physicochemical reaction between the biochar surface groups and the heavy metals in the water sample. The SBC600 had higher adsorption performance (Que *et al*. 2018). The SBC tended to be fragmented at 700 °C. This situation was caused by excessive temperature that damaged the porous structure to some extent, and might have reduced the adsorption performance of SBC700.

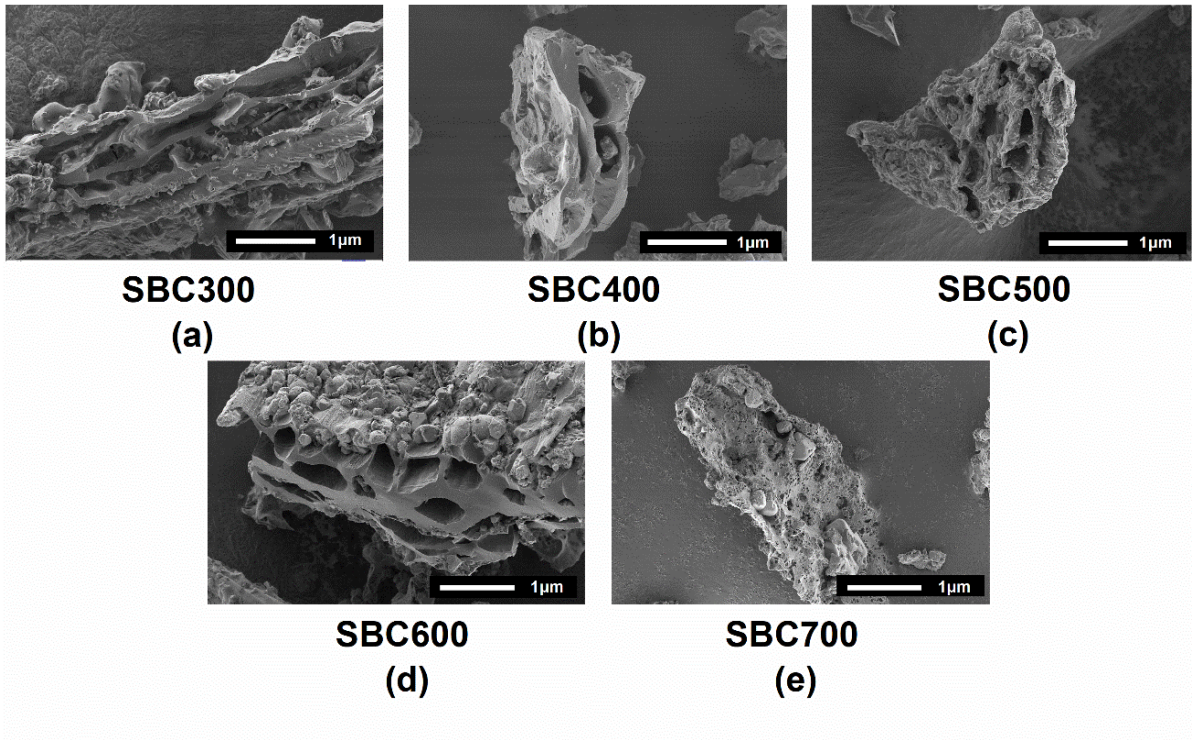

Fig. 2. SEM of biochar at different pyrolysis temperatures

Elemental analysis

Elemental analysis of biochar is an important method to judge its structure and properties (Enders and Lehmann 2012). As the preparation temperature increased, the carbon (C) and sulfur (S) content in the SBC increased, while the content of hydrogen (H), nitrogen (N), and oxygen (O) decreased (Table 2). The study of peanut shell and Chinese medicine residue biochar had a similar regular pattern (Boni *et al*. 2018). During pyrolysis, the increase of C content was attributed to the degree of carbonization of SBC that increased as the temperature of the preparation increased. The reduction in H, N, and O content might be due to dehydration of the dross material and breakage of weak bonds in

the structure (Boni *et al.* 2018). At the same time, when the preparation temperature rose from 300 °C to 700 °C, the content ratio of N/C decreased from 0.08 to 0.04, and the content ratio of H/C decreased from 0.10 to 0.04, while the content ratio of O/C decreased from 0.14 to 0.11.

The content ratio of H/C is often used to characterize the aromaticity of biochar. It was more stable in the environment when the aromaticity was higher (Wang *et al.* 2014). The gradual decrease of the content ratio of H/C indicated that the degree of aromatization increased when the preparation temperature increased, and the SBC600 and SBC700 had higher stability in the environment (Ferralis *et al*. 2015). This is consistent with the changes of the content ratios of H/C of bamboo biochar studied by Chen *et al*. (2016). The content ratio of O/C can be used to estimate the polarity of the biochar (Chen *et al*. 2016). When the value was higher, the polarity was greater. With the increase of the preparation temperature, the content ratio of O/C did not change remarkably and then decreased, indicating that the polarity of SBC and the number of polar functional groups decreased as the preparation temperature reached 600 °C. The non-polarity of biochar was stronger when it was more stable (Wang *et al*. 2014; Samsuri *et al*. 2014). Therefore, SBC600 and SBC700 had long-term stability in the environment.

Table 2. Elemental Composition of Biochar at Different Pyrolysis Temperatures

Preparation Temperature (°C)	Elemental Composition (%)					Content Ratio of Element		
	C	H	N	O	S	O/C	N/C	H/C
300	75.59	7.50	5.85	10.88	0.18	0.14	0.08	0.10
400	77.21	7.04	4.70	10.87	0.23	0.14	0.06	0.09
500	78.73	6.55	3.80	10.74	0.30	0.14	0.05	0.08
600	81.69	5.14	2.88	10.10	0.32	0.12	0.04	0.06
700	83.80	3.60	2.97	9.44	0.35	0.11	0.04	0.04

Effects of Solution pH

The adsorption of heavy metal ions by biochar was closely related to the pH of the solution (Ma *et al*. 2014; Ahmed *et al*. 2016). When the pH was raised from 1 to 6, the removal rates and adsorption capacities of Cr^{6+} by SBC600 decreased, the removal rates of Pb^{2+} increased, and the adsorption capacities of Pb^{2+} gradually decreased (Fig. 3). When the pH of the solution was 1.0, SBC600 had the highest removal rate of Cr^{6+} by SBC600 (82.5%). When the pH was raised from 1.0 to 3.0, the removal rates of Cr^{6+} by SBC600 reduced 71.7% compared with that of pH 1.0, and the adsorption capacities also significantly decreased ($P < 0.05$). When the pH > 3.0, the capacities of Cr^{6+} by SBC showed no significant change ($P > 0.05$), or tended to be stable. When the pH was 3 to 4, the removal rates of Pb^{2+} increased significantly ($P < 0.05$), and the adsorption capacities decreased the fastest. When the pH was raised from 4 to 6, the growth rate of removal rates for Pb^{2+} slowly increased and the rate of decrease of adsorption capacities slowly decreased. When pH was 6.0, the removal rate (96.0%) and adsorption capacity (13.29 mg/g) reached

a steady state. This might have been because Pb^{2+} was generally present in the aqueous solution in the form of ions under the acidic condition. Therefore, the adsorption effect of biochar was poor, and when the pH was further increased, Pb^{2+} would bind to the hydroxyl group in the solution, and precipitation would occur, thereby noticeably increasing the adsorption effect of biochar (Liang *et al.* 2009).

The two main reasons why the adsorption of metal ions was affected by the acidity of the solution are the acid-base and the zero-charge sites (Nassar 2010). When the pH raised from 3 to 4, the adsorption capacities of SBC600 for Pb^{2+} increased greatly. On the one hand, the functional group sites on the surface of the adsorbent (mainly were carboxylate groups) and a large number of H^+ and conjugated points of π in the solution competed with Pb^{2+} for adsorption, and the cations occupied the main position of the adsorbent surface and inhibited the adsorption of adsorbent (Liu and Zhang 2009). In contrast, excess H^+ in the solution formed a positive group on the protonated surface of SBC600, and repelled Pb^{2+} ions that were positively charged (Xu *et al*. 2015). When the pH raised from 3 to 4, the adsorption capacities decreased as the adsorption capacities of the acidic functional groups on the surface of the adsorbent and the surface negative charge decreased (Xu *et al*. 2013).

The difference of Cr^{6+} removal rates and adsorption capacities under different solution pH might be due to the influence of pH on the surface functional group state of the adsorbent (Contreras *et al*. 2009). Meanwhile, the pH influenced the ionic species of Cr present, and this was also affected by the redox potential in the system, which can change due to oxidation of biomass on by the presence of oxygen from the air. Factors of importance include the concentration of H^+, the species of Cr, and their distributions in the system (Feng *et al*. 2006). With the participation of H^+, the protonated adsorption sites formed on the surface of SBC increased. At this time, Cr^{6+} mainly existed in the form of CrO_4^{2-}, $HCrO_4^-$, and $Cr_2O_7^{2-}$. These ions were easily adsorbed to the protonated binding adsorption site *via* electrostatic attraction (Ma *et al*. 2012). With the increase of pH, the increase of negative charge on the surface of biochar had a certain rejection effect on $Cr_2O_7^{2-}$, which was not conducive to the reaction (Park *et al*. 2008). The ionic radius increased as the proportion of Cr^{6+} in the form of CrO_4^{2-} in the solution increased, resulting in the repellency of the adsorbent on CrO_4^{2-} (Xue *et al.* 2016). Therefore, the existence form of Cr^{6+} under low pH conditions was more suitable for physical adsorption, like electrostatic attraction to the SBC surface. Zhu *et al*. (2016) previously reported similar findings.

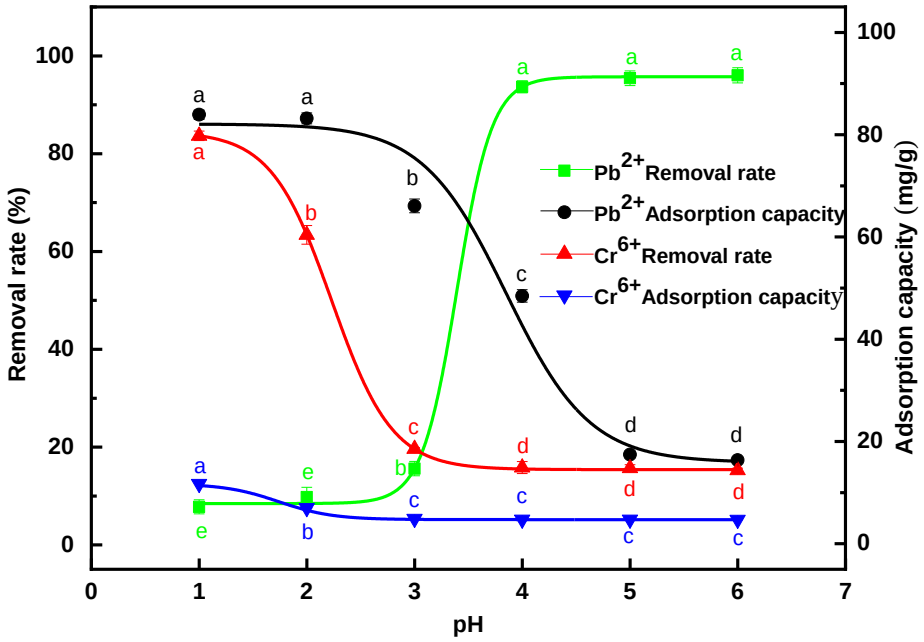

Fig. 3. Effect of pH on Pb^{2+} and Cr^{6+} removal rate and adsorption capacity

Kinetics of Cr^{6+} and Pb^{2+} Adsorption on SBC600

Reaction time is a key factor affecting the adsorption process (Zhu *et al*. 2016). With the increase of adsorption time, the removal rates and adsorption capacities of Cr^{6+} by SBC600 increased first and then stabilized (Fig. 4). After a 2 h adsorption, the change of removal rates and the adsorption capacities of Cr^{6+} showed no significance ($P > 0.05$). This result indicated that the adsorption had reached equilibrium. At first, SBC600 adsorbed a large amount of Cr^{6+} through the surface pores. It was physical adsorption at this stage, and the adsorption was fast. After a period of time, the adsorption tended to be saturated, mainly characterized by chemisorption that was slow (Xi *et al*. 2016). The time for biochar to achieve adsorption equilibrium for adsorption of Cr^{6+} was closely related to the raw materials of biochar. For example, the adsorption equilibrium time of corn cob biochar is 4 h (Hua *et al*. 2012), and the adsorption of banana pseudostem biochar might not reach equilibrium within 48 h (Xu *et al*. 2018), while the adsorption time of SBC600 for Cr^{6+} was only 2 h, indicating that the adsorption of SBC600 was efficient and so it had a great advantage in the adsorption of Cr^{6+} in wastewater.

When the initial concentration of Pb^{2+} was 100 mg/L, the removal rate of Pb^{2+} was 93.1% after 20 min of adsorption. When the adsorption duration was 24 h, the adsorption reached equilibrium, and the removal rate of Pb^{2+} was 96.7%. After adsorbing for 5 min, the adsorption capacity was lower than the saturated adsorption capacity, indicating that the adsorption rate of Pb^{2+} was slow, and the adsorption equilibrium could be reached at 24 h. This result could have been attributed to the adsorption process being divided into two stages. The first stage was rapid adsorption, mainly controlled by physical adsorption, Pb^{2+} ions quickly occupied the adsorption sites on the surface of the solution and slowly adsorbed in the second stage that was mainly dominated by chemical adsorption (Tang *et al*. 2016).

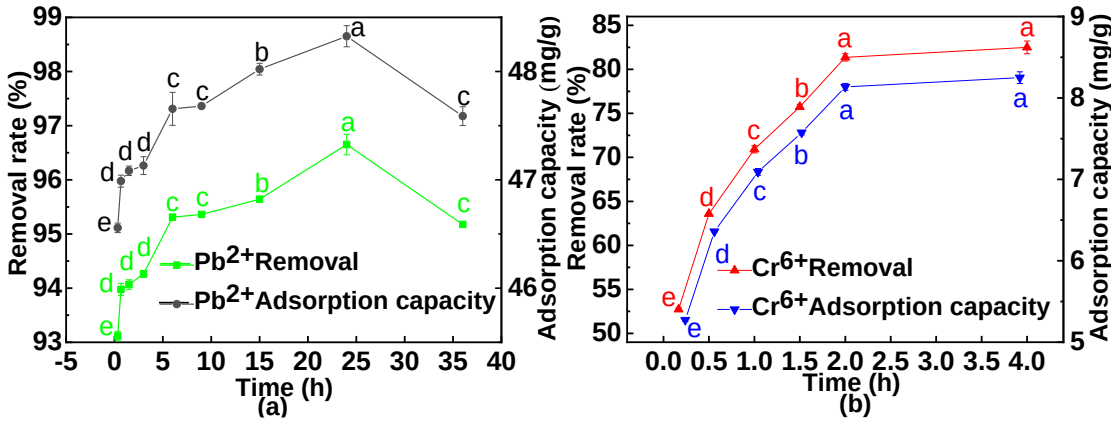

Fig. 4. Kinetics of SBC600 adsorption on Cr^{6+} and Pb^{2+}

To further study the kinetic adsorption characteristics of SBC600, the adsorption kinetic that could fit well with data was selected. From the results shown in Table 3, when the pseudo-first-order kinetic model was used to fit, the R^2 was closer to 1, and the saturation adsorption capacity obtained by fitting the data was in good agreement with the actual data. This indicated that the model could describe the adsorption process of Cr^{6+} and Pb^{2+} by SBC better. The interaction between metal ions (Cr^{6+} and Pb^{2+}) and SBC might be ion exchange, share of the electron pair, surface precipitation or surface complexation. Compared with adsorbents previously reported in biochar for Cr^{6+}, such as hazelnut shell and cow dung, and biochar for Pb^{2+}, such as orange peel and modified litchi peel (Kobya 2004; Singh and Rattan 2014; Jiang *et al*. 2015; Abbaszadeh *et al*. 2016). It was found that when SBC adsorbed Cr^{6+} and Pb^{2+}, the equilibrium of the water solution maintained for a long time, and its adsorption capacity was noticeably higher.

Table 3. Kinetics Fitting Parameters of SBC600 Adsorption on Cr^{6+} and Pb^{2+}

Heavy Metal Species	Initial Concentration C_0 (mg/L)	Pseudo-first-order Kinetic Model			Pseudo-second-order Kinetic Model		
		q_e (mg/g)	K_1 (/min)	R^2	q_e (mg/g)	K_2 (g/(mg·min))	R^2
Cr^{6+}	50	7.44	0.11	0.959	8.49	0.017	0.998
Pb^{2+}	100	47.52	0.19	0.284	47.82	1.141	0.999

Isotherm of Cr^{6+} and Pb^{2+} Adsorption on SBC600

The adsorption effect of biochar under different initial concentration conditions of heavy metal could reflect its adsorption performance to some extent (Abdelhafez and Li 2016). Figure 5 shows that the adsorption capacities of Pb^{2+} by SBC600 gradually increased as the initial concentration increased. This phenomenon might be due to the fact that when the initial concentration of the solution was low, the adsorbent could provide sufficient adsorption sites and active groups (Abdelhafez and Li 2016).

At the same time, with the increase of the initial concentration of the solution, the removal rates of Cr^{6+} by SBC gradually decreased (Fig. 5). When the initial concentration of the solution was 50 mg/L, the removal rate of Cr^{6+} by SBC600 could reach 82.5%, indicating that the adsorption effect was excellent. With the increase of the initial

concentration of the solution, the adsorption capacities of SBC for Cr^{6+} increased, reached the maximum value of 10.01 mg/g at the concentration of 125 mg/L, and then stabilized. When the concentration of the solution continued to increase, the increase in the equilibrium adsorption capacities slowed down, and gradually tended to the balanced state of adsorption capacities. Because of the increase of the solution concentration, the number of parts on SBC600 that could adsorb Cr^{6+} was gradually reduced so that the adsorbent gradually reached the adsorption saturation state.

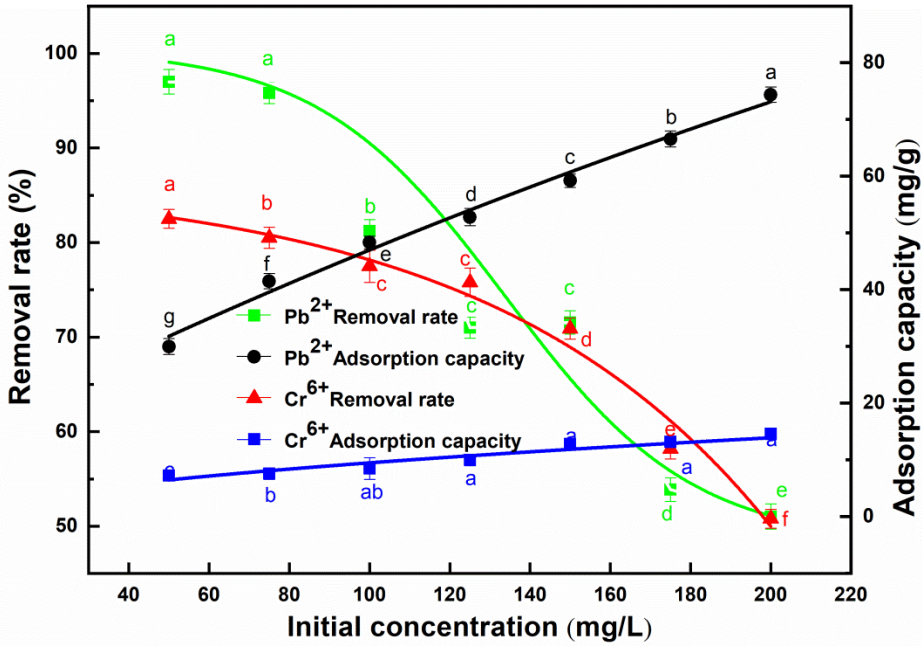

Fig. 5. Isotherm of SBC600 adsorption on Cr^{6+} and Pb^{2+}

The adsorption isotherm can reflect the characteristics of adsorption strength, adsorption capacity, and adsorption state, and describes the equilibrium relationship between the adsorbent and adsorbate (Li *et al*. 2018). The adsorption isotherms of Pb^{2+} and Cr^{6+} of SBC at 25 °C accorded with the Freundlich and Langmuir equations. The fitting results of each parameter are shown in Table 4. The R^2 of the Langmuir equation was larger, and the saturated adsorption capacity calculated was closer to the experimental data. Therefore, the Langmuir equation was more suitable for the isothermal adsorption process of Pb^{2+} and Cr^{6+} by SBC600. The Langmuir equation assumed that the adjacent adsorption sites did not affect each other. Therefore, the adsorption process of SBC600 fitted the ideal monolayer adsorption model, mainly characterized by monolayer adsorption (Park *et al*. 2016; Tran *et al*. 2016). Another study by Wang *et al.* (2018b) had also reached similar conclusions that the adsorption equilibrium of Pb^{2+} from aqueous solutions on biochar produced from *Phytolacca americana* L. biomass was best described by Langmuir isotherms. It could be calculated from the relevant formula that the values of K_L on SBC for Pb^{2+} and Cr^{6+} adsorption in the Langmuir equation were 0.0022 to 0.0060 (between 0 and 1), indicating that the adsorption was the favorable adsorption.

The theoretical maximum adsorption capacity of SBC600 on Cr^{6+} and Pb^{2+} by the Langmuir equation was 25.80 mg/g and 135.3 mg/g, respectively. The maximum adsorption capacity of Cr^{6+} was higher than that of activated carbon (19.31 mg/g), but a bit lower than protonated titanate nanotubes (26.60 mg/g), and the maximum adsorption

capacity of Pb^{2+} was higher than that of coffee husk biomass waste (37.04 mg/g) (Wang *et al*. 2013; Wang *et al*. 2016; Wang *et al*. 2018c; Alhogbi 2017). The comparison indicated that SBC600 had certain potentials for adsorption of Cr^{6+} and Pb^{2+}.

Table 4. Isotherm Fitting Parameters of SBC600 Adsorption on Cr^{6+} and Pb^{2+}

Heavy Metal Ion	Temperature (°C)	Langmuir Equation			Freundlich Equation		
		Q_m (mg/g)	K_L (L/mg)	R^2	K_f (mg/g)	n	R^2
Cr^{6+}	25	25.80	0.0059	0.913	0.8845	1.817	0.904
Pb^{2+}		135.3	0.0055	0.957	1.427	1.615	0.947

CONCLUSIONS

1. The FTIR, SEM, and elemental analysis showed that with the increase of pyrolysis temperature, the average pore diameter of biochar increased, the pore structure developed, micropores formed, and the pore volume and specific surface area increased, accordingly. The alkyl group was missing, and the degree of aromatization and stability of SBC600 and SBC700 were enhanced, which was beneficial to the adsorption of heavy metals.
2. Factors, such as the initial pH of solution, the initial concentration of heavy metal, and adsorption time, were related to the adsorption effect of SBC by batch adsorption experiments. The appropriate values of pH were 1.0 for Cr^{6+} and 4.0 for Pb^{2+}. The maximum adsorption capacities were 25.8 mg/g for Cr^{6+} and 135.3 mg/g for Pb^{2+}.
3. Data was fitted with the kinetic equation and isotherm equation to understand the adsorption process and mechanism. The pseudo-second-order kinetic model ($R^2 > 0.997$) and Langmuir equation ($R^2 > 0.912$) described the process of SBC adsorption of Cr^{6+} and Pb^{2+} better.
4. The SBC effectively adsorbed Cr^{6+} and Pb^{2+} in aqueous solution under appropriate conditions, which means SSR is a biochar material with certain potential for heavy metals removal.

ACKNOWLEDGMENTS

The authors are grateful for the support of Key Research and Development Projects of Sichuan Province, China, Grant No. 19ZDYF2427.

REFERENCES CITED

Abbaszadeh, S., Alwi, S. R. W., Webb, C., Ghasemi, N., and Muhamad, I. I. (2016). "Treatment of lead-contaminated water using activated carbon adsorbent from locally available papaya peel biowaste," *J. Clean. Prod.* 118, 210-222. DOI: 10.1016/j.jclepro.2016.01.054

Abdelhafez, A. A., and Li, J. (2016). "Removal of Pb (II) from aqueous solution by using biochars derived from sugar cane bagasse and orange peel," *J. Taiwan Inst. Chem. E.* 61, 367-375. DOI: 10.1016/j.jtice.2016.01.005

Ahmed, M. B., Zhou, J. L., Ngo, H. H., and Guo, W. (2016). "Insight into biochar properties and its cost analysis," *Biomass Bioenerg.* 84, 76-86. DOI: 10.1016/j.biombioe.2015.11.002

Alhogbi, B. G. (2017). "Potential of coffee husk biomass waste for the adsorption of Pb (II) ion from aqueous solutions," *Sustainable Chemistry and Pharmacy* 6, 21-25. DOI: 10.1016/j.scp.2017.06.004

Amin, M. T., Alazba, A. A., and Shafiq, M. (2017). "Removal of copper and lead using banana biochar in batch adsorption systems: Isotherms and kinetic studies," *Arab. J. Sci. Eng*. 43(11), 5711-5722. DOI: 10.1007/s13369-017-2934-z

Boni, M., Chiavola, A., and Marzeddu, S. (2018). "Application of biochar to the remediation of Pb-contaminated solutions," *Sustainability* 10(12), Article ID 4440. DOI: 10.3390/su10124440

Brahmi, K., Bouguerra, W., and Harbi, S. (2017). "Treatment of heavy metal polluted industrial wastewater by a new water treatment process ballasted electroflocculation," *J. Hazard. Mater.* 344, 968-980. DOI: 10.1016/j.jhazmat.2017.11.051

Chen, D., Yu, X., Song, C., Pang, X., Huang, J., and Li, Y. (2016). "Effect of pyrolysis temperature on the chemical oxidation stability of bamboo biochar," *Bioresource Technol.* 218, 1303-1306. DOI: 10.1016/j.biortech.2016.07.112

Chen, J., Yang, P., Song, D., Yang, S., Zhou, L., Han, L., and Lai, B. (2014a). "Biosorption of Cr (VI) by carbonized *Eupatorium adenophorum* and Buckwheat straw: Thermodynamics and mechanism," *Front. Env. Sci. Eng.* 8(6), 960-966. DOI: 10.1007/s11783-013-0612-2

Chen, X., Luo, Y., Qi, B., and Wan, Y. (2014b). "Simultaneous extraction of oil and soy isoflavones from soy sauce residue using ultrasonic-assisted two-phase solvent extraction technology," *Sep. Purif. Technol.* 128, 72-79. DOI: 10.1016/j.seppur.2014.03.014

Contreras, M., Lagos, G., Escalona, N., Soto-Garrido, G., Radovic, L. R., and Garcia, R. (2009). "On the methane adsorption capacity of activated carbons: In search of a correlation with adsorbent properties," *J. Appl. Chem. Biotechn.* 84(11), 1736-1741. DOI: 10.1002/jctb.2239

Diao, Z. H., Du, J. J., Jiang, D., Kong, L. J., Huo, W. Y., Liu, C. M., Wu, Q. H., and Xu, X. R. (2018). "Insights into the simultaneous removal of Cr^{6+} and Pb^{2+} by a novel sewage sludge-derived biochar immobilized nanoscale zero valent iron: Coexistence effect and mechanism," *Sci. Total Environ.* 642, 505-515. DOI: 10.1016/j.scitotenv.2018.06.093

Duan, Y., Zhou, A., Wen, K., Liu, Z., Liu, W., Wang, A., and Yue, X. (2019). "Upgrading VFAs bioproduction from waste activated sludge *via* co-fermentation with soy sauce residue," *Front. Env. Sci. Eng* 13(1), 1-10. DOI: 10.1007/s11783-019-1086-7

Enders, A., and Lehmann, J. (2012). "Comparison of wet-digestion and dry-ashing methods for total elemental analysis of biochar," *Commun. Soil Sci. Plan. Anal* 43(7), 1042-1052. DOI: 10.1080/00103624.2012.656167

Fan, S., Li, H., Wang, Y., Wang, Z., Tang, J., Tang, J., and Li, X. (2018). "Cadmium removal from aqueous solution by biochar obtained by co-pyrolysis of sewage sludge

with tea waste," *Res. Chem. Intermediat.* 44(1), 135-154. DOI: 10.1007/s11164-017-3094-1

Ferralis, N., Liu, Y., Bake, K. D., Pomerantz, A. E., and Grossman, J. C. (2015). "Direct correlation between aromatization of carbon-rich organic matter and its visible electronic absorption edge," *Carbon* 88, 139-147. DOI: 10.1016/j.carbon.2015.02.075

Feng, X. H., Zhai, L. M., Tan, W. F., Zhao, W., Liu, F., and He, J. Z. (2006). "The controlling effect of pH on oxidation of Cr(III) by manganese oxide minerals," *J. Colloid Interface Sci. 298*(1), 258-266. DOI: 10.1016/j.jcis.2005.12.012

Guan, X., and Sun, L. N. (2014). "Current situation and the harm of soil heavy metal pollution and food safety," *Appl. Mech. Mater.* 675-677, 612-614. DOI: 10.4028/www.scientific.net/AMM.675-677.612

Hamza, U. D., Nasri, N. S., Amin, N. S., Mohammed, J., and Zain, H. M. (2016). "Characteristics of oil palm shell biochar and activated carbon prepared at different carbonization times," *Desalin. Water Treat.* 57(17), 7999-8006. DOI: 10.1080/19443994.2015.1042068

Hua, C., Zhang, R., Li, L., and Zheng, X. (2012). "Adsorption of phenol from aqueous solutions using activated carbon prepared from crofton weed," *Desalin. Water Treat.* 37(1-3), 230-237. DOI: 10.1080/19443994.2012.661277

Izah, S. C., Chakrabarty, N., and Srivastav, A. L. (2016). "A review on heavy metal concentration in potable water sources in Nigeria: Human health effects and mitigating measures," *Expos. Health* 8(2), 285-304. DOI: 10.1007/s12403-016-0195-9

Jiang, R., Tian, J., Zheng, H., Qi, J., Sun, S., and Li, X. (2015). "A novel magnetic adsorbent based on waste litchi peels for removing Pb (II) from aqueous solution," *J. Environ. Manage.* 155, 24-30. DOI: 10.1016/j.jenvman.2015.03.009

Kiran, M. G., Pakshirajan, K., and Das, G. (2017). "An overview of sulfidogenic biological reactors for the simultaneous treatment of sulfate and heavy metal rich wastewater," *Chem. Eng. Sci.* 158, 606-620. DOI: 10.1016/j.ces.2016.11.002

Kobya, M. (2004). "Removal of Cr(VI) from aqueous solutions by adsorption onto hazelnut shell activated carbon: Kinetic and equilibrium studies," *Bioresource Technol.* 91(3), 317-321. DOI: 10.1016/j.biortech.2003.07.001

Lammers, K., Arbuckle-Keil, G., and Dighton, J. (2009). "FT-IR study of the changes in carbohydrate chemistry of three New Jersey pine barrens leaf litters during simulated control burning," *Soil Biol. Biochem.* 41(2), 340-347. DOI: 10.1016/j.soilbio.2008.11.005

Lee, S. J., Park, J. H., Ahn, Y. T., and Chung, J. W. (2015). "Comparison of heavy metal adsorption by peat moss and peat moss-derived biochar produced under different carbonization conditions," *Water Air Soil Poll.* 226, Article ID 9. DOI: 10.1007/s11270-014-2275-4

Li, S., Zhu, D., Li, K., Yang, Y., Lei, Z., and Zhang, Z. (2013). "Soybean curd residue: Composition, utilization, and related limiting factors," *ISRN Industrial Engineering* 2013, Article ID 423590. DOI: 10.1155/2013/423590

Li, Y., Wei, Y., Huang, S., Liu, X., Jin, Z., Zhang, M., Qu, J. J., and Jin, Y. (2018). "Biosorption of Cr (VI) onto *Auricularia auricula* dreg biochar modified by cationic surfactant: Characteristics and mechanism," *J. Mol. Liq.* 269, 824-832. DOI: 10.1016/j.molliq.2018.08.060

Liang, S., Guo, X. Y., Feng, N. C., and Tian, Q. H. (2009). "Adsorption of Cu^{2+} and Cd^{2+} from aqueous solution by mercapto-acetic acid modified orange peel," *Colloid. Surface. B* 73(1), 10-14. DOI: 10.1016/j.colsurfb.2009.04.021

Liu, Z., and Zhang, F. S. (2009). "Removal of lead from water using biochars prepared from hydrothermal liquefaction of biomass," *J. Hazard. Mater.* 167(1-3), 933-939. DOI: 10.1016/j.jhazmat.2009.01.085

Ma, J., Yu, F., Zhou, L., Jin, L., Yang, M., Luan, J., Tang, Y. H., Fan, H. B., Yuan, Z. W., and Chen, J. H. (2012). "Enhanced adsorptive removal of methyl orange and methylene blue from aqueous solution by alkali-activated multiwalled carbon nanotubes," *ACS Appl. Mater. Inter.* 4(11), 5749-5760. DOI: 10.1021/am301053m

Ma, Y., Liu, W. J., Zhang, N., Li, Y. S., Jiang, H., and Sheng, G. P. (2014). "Polyethylenimine modified biochar adsorbent for hexavalent chromium removal from the aqueous solution," *Bioresource Technol* 169, 403-408. DOI: 10.1016/j.biortech.2014.07.014

Meng, X. M., Wan, Y. L., Feng, K., Kong, H. Z., and Liu, T. Z. (2019). "Preparation and characteristics of three sorbents from wood chips screening reject (WCSR) modified by nitric acid, phosphoric acid, or sodium hydroxide," *BioResources* 14(1), 2216-2228. DOI: 10.15376/biores.14.1.2216-2228

Nassar, N. N. (2010). "Rapid removal and recovery of Pb (II) from wastewater by magnetic nanoadsorbents," *J. Hazard. Mater.* 184(1-3), 538-546. DOI: 10.1016/j.jhazmat.2010.08.069

Park, D., Lim, S. R., Yun, Y. S., and Park, J. M. (2008). "Development of a new Cr (VI)-biosorbent from agricultural biowaste," *Bioresource Technol.* 99(18), 8810-8818. DOI: 10.1016/j.biortech.2008.04.042

Park, J. H., Cho, J. S., Ok, Y. S., Kim, S. H., Heo, J. S., Delaune, R. D., and Seo, D. C. (2016). "Comparison of single and competitive metal adsorption by pepper stem biochar," *Arch. Agron. Soil Sci.* 62(5), 617-632. DOI: 10.1080/03650340.2015.1074186

Que, W., Zhou, Y. H., Liu, Y. G., Wen, J., Tan, X. F., Liu, S. J., and Jiang, L. H. (2018). "Appraising the effect of *in-situ* remediation of heavy metal contaminated sediment by biochar and activated carbon on Cu immobilization and microbial community," *Ecol. Eng.* 127, 519-526. DOI: 10.1016/j.ecoleng.2018.10.005

Radwan, A. A., Alanazi, F. K., and Alsarra, I. A. (2010). "Microwave irradiation-assisted synthesis of a novel crown ether crosslinked chitosan as a chelating agent for heavy metal ions (M + n)," *Molecules* 15(9), 6257-6268. DOI: 10.3390/molecules15096257

Samsuri, A. W., Sadegh-Zadeh, F., and Seh-Bardan, B. J. (2014). "Characterization of biochars produced from oil palm and rice husks and their adsorption capacities for heavy metals," *Int. J. Environ. Sci. Te* 11(4), 967-976. DOI: 10.1007/s13762-013-0291-3

Shaw, D. R., and Dussan, J. (2017). "Transcriptional analysis and molecular dynamics simulations reveal the mechanism of toxic metals removal and efflux pumps in *Lysinibacillus sphaericus* OT4b.31," *Int. Biodeter. Biodegradr.* 127, 46-61. DOI: 10.1016/j.ibiod.2017.11.016

Singh, H., and Rattan, V. K. (2014). "Comparison of hexavalent chromium adsorption from aqueous solutions by various biowastes and granulated activated carbon," *Indian Chemical Engineer* 56(1), 12-28. DOI: 10.1080/00194506.2014.881002

Tang, S., Chen, Y., Xie, R., Jiang, W., and Jiang, Y. (2016). "Preparation of activated carbon from corn cob and its adsorption behavior on Cr (VI) removal," *Water Sci. Technol.* 73(11), 2654-2661. DOI: 10.2166/wst.2016.120

Tran, H. N., You, S. J., and Chao, H. P. (2016). "Thermodynamic parameters of cadmium adsorption onto orange peel calculated from various methods: A comparison study," *J. Environ. Chem. Eng.* 4(3), 2671-2682. DOI: 10.1016/j.jece.2016.05.009

Wang, H. H., Wang, X., Cui, Y. S., Xue, Z. C., and Ba, Y. X. (2018a). "Slow pyrolysis polygeneration of bamboo (*phyllostachys pubescens*): Product yield prediction and biochar formation mechanism," *Bioresour. Technol.* 263(27), 19065-19078. DOI: 10.1016/j.biortech.2018.05.040

Wang, G. Y., Zhang, S. R., Yao, P., Chen, Y., Xu, X., Li, T., and Gong, G. S. (2018b). "Removal of Pb(II) from aqueous solutions by *Phytolacca americana* L. biomass as a low cost biosorbent," *Arabian Journal of Chemistry* 11(1), 99-110. DOI: 10.1016/j.arabjc.2015.06.011

Wang, L., Liu, W., Wang, T., and Ni, J. (2013). "Highly efficient adsorption of Cr (VI) from aqueous solutions by amino-functionalized titanate nanotubes," *Chem. Eng. J.* 225, 153-163. DOI: 10.1016/j.cej.2013.03.081

Wang, W. L., Liu, Y., Liu, X. H., Deng, B. J, Lu, S. Y, Zhang, Y. R., Bi, B., and Ren, Z. M. (2018c). "Equilibrium adsorption study of the adsorptive removal of Cd^{2+} and Cr^{6+} using activated carbon," *Environ. Sci. Pollut. R.* 25(25), 25538-25550. DOI: 10.1007/s11356-018-2635-5

Wang, Z. Y., Liu, G. C., Monica, X., Li, F. M., and Zheng, H. (2014). "Adsorption of Cd (II) varies with biochars derived at different pyrolysis temperatures," *Environmental Science* 35(12), 4735-4744. (In Chinese) DOI: 10.13227/j.hjkx.2014.12.042

Wu, Y., Cha, L., Fan, Y., Fang, P., and Sha, H. (2017). "Activated biochar prepared by pomelo peel using H_3PO_4 for the adsorption of hexavalent chromium: performance and mechanism. *Water Air Soil Poll.* 228(10), Article ID 405. DOI: 10.1007/s11270-017-3587-y

Xi, J., He, M., and Kong, L. (2016). "Adsorption of antimony on kaolinite as a function of time, pH, HA and competitive anions," *Environ. Earth Sci.* 75(2), Article ID 136. DOI: 10.1007/s12665-015-4916-3

Xu, S., Yu, W., Liu, S., Xu, C., Li, J., and Zhang, Y. (2018). "Adsorption of hexavalent chromium using banana pseudostem biochar and its mechanism," *Sustainability* 10(11), Article ID 4250. DOI: 10.3390/su10114250

Xu, X., Cao, X., Zhao, L., Wang, H., Yu, H., and Gao, B. (2013). "Removal of Cu, Zn, and Cd from aqueous solutions by the dairy manure-derived biochar," *Environ. Sci. Pollut. R.* 20(1), 358-368. DOI: 10.1007/s11356-012-0873-5

Xu, Y., Dang, Q., Liu, C., Yan, J., Fan, B., Cai, J., and Li, J. (2015). "Preparation and characterization of carboxyl-functionalized chitosan magnetic microspheres and submicrospheres for Pb^{2+} removal," *Colloid. Surface. A* 482, 353-364. DOI: 10.1016/j.colsurfa.2015.06.028

Xue, Y., Qian, L., Sui, J. C., Gao, W. G., Chen, M. Y., Cao, Z. Q., and Schweilin (2016). "Removal of Cr(VI) from aqueous using biochar carried nanoscal zero-velent iron," *Chinese Journal of Environmental Engineering* 10(6), 2895-2901. DOI: 10.12030/j.cjee.201501155

Zhang, D. L., Zhang, M., Zhang, C., Sun, Y., Sun, X., and Yuan, X. (2016). "Pyrolysis treatment of chromite ore processing residue by biomass: Cellulose pyrolysis and Cr (VI) reduction behavior," *Environ. Sci. Technol.* 50(6), 3111-3118. DOI: 10.1021/acs.est.5b05707

Zhang, W., Mao, S., Chen, H., Huang, L., and Qiu, R. (2013). "Pb(II) and Cr(VI) sorption by biochars pyrolyzed from the municipal wastewater sludge under different

heating conditions," *Bioresource Technol.* 147, 545-552. DOI: 10.1016/j.biortech.2013.08.082

Zhu, Q., Wu, J., Wang, L., Yang, G., and Zhang, X. (2016). "Adsorption characteristics of Pb^{2+} onto wine lees-derived biochar," *B. Environ. Contam. Tox.* 97(2), 294-299. DOI: 10.1007/s00128-016-1760-4

Article submitted: March 22, 2019; Peer review completed: April 12, 2019; Revisions received: April 17, 2019; Revisions accepted: April 22, 2019; Published: April
DOI: 10.15376/biores.14.2.4653-4669